Theoretical Study on Nonreciprocity for Third-Harmonic Generation Process in Nonlinear Photonic Crystals

Dongrui Di, Binglin Zhang, Jiaying Wang, and Ronger Lu

***Abstract*—Based on the nonlinear coupled wave equations, the nonreciprocal response of the third-harmonic generation process has been theoretically investigated in nonlinear photonic crystals with a defect embedded. The simulation results have shown that complete nonreciprocity for third-harmonic generation can be achieved under specific conditions, and the arbitrary nonreciprocal response can be realized by adjusting the structure parameters, including the crystal length, the defect position and the defect width. These findings hold great potential for implementing practical nonlinear optical isolating devices.**

***Index Terms*—Nonreciprocity, third-harmonic-generation, nonlinear photonic crystals, optical isolators.**

I. Introduction

NONRECIPROCAL effect is an important basic concept in many fields including electricity, acoustics and optics. It is an asymmetric transmission, which means that the wave transmits in the opposite two directions in a certain material with different energy properties and phase shifts. In recent years, inspired by the electrical asymmetry of diodes [1], [2], [3], the study of nonreciprocal processes in various physical systems has gradually become a hot issue. For example, a non-Hermitian topology circuit with nonreciprocal effect was constructed, showing the phenomenon of inconsistent energy band structure under open boundary conditions and periodic boundary conditions [4]. A space-time modulated acoustic metamaterial was designed, which realized effective nonreciprocal modal transition [5]. In the field of optics, there are various structures and methods that can achieve nonreciprocity. A complex short-period (Bragg) grating was designed to realize asymmetrical mode coupling within a contra-directional waveguide coupler [6]. A metal-silicon waveguide system was designed to realize the nonreciprocal transmission of light waves on silicon wafers [7]. An approach of magnetic-free nonreciprocity by optically-induced magnetization in an atom ensemble was put forward [8].

In nonlinear optics, nonreciprocity can be achieved by many methods. For example, nonlinearities in the form of stimulated Raman scattering [9], [10], stimulated Brillouin scattering [11], [12], [13], [14] or four-wave mixing effect [15], [16], [17], [18] were used to achieve nonreciprocal operation. Optical isolators, circulators, and amplifiers based on these effects were further designed to dynamically reconfigure isolation direction. An optical diode-like acting structure was obtained by utilizing chirped photonic crystals [19]. The performance of optical isolator could be adjusted by changing external electric field in periodically poled lithium niobate ($LiNbO_3$, LN) with defects [20]. The implementation conditions of different nonreciprocal parameters were further studied in these structures [21].

These studies reported a variety of nonlinear nonreciprocity, but there is little work focused on third-harmonic generation (THG). In this paper, we theoretically studied the nonreciprocity in the coupled THG process based on one-dimension (1D) nonlinear photonic crystal (NPC) structures with defects. The forward and backward harmonic evolution diagrams were obtained corresponding to the original equations and the simplified equations. It can be found from the simulations that complete nonreciprocity can be achieved in THG process. Various degrees of nonlinear nonreciprocity for THG can be obtained by changing the crystal length, defect position and defect width. This has potential applications in the design of all-optical diodes, optical isolators, amplifiers, and circulators.

II. THG Simulations for Forward and Backward Transmission Processes

We have already known that the introduction of the defect in the periodic 1D NPC structures can excite nonreciprocal response in the second harmonic generation (SHG) process [22], [23]. In fact, this method is designed to make NPCs into asymmetric structures, and the introduction of defects causes a sudden phase shift in the coupled wave equations, resulting in the fluctuation of the final solution of harmonic waves. Inspired by this, we can also achieve the nonreciprocity for the THG process by adding a defect in chirped NPCs. A non-centrosymmetric

Manuscript received 20 February 2023; revised 2 April 2023; accepted 12 April 2023. Date of publication 20 April 2023; date of current version 30 April 2023. This work was supported in part by the National Natural Science Foundation of China under Grant 12004177, in part by the Natural Science Foundation of Jiangsu Province under Grant BK20200701, in part by the Innovation and Entrepreneurship Program of Jiangsu Province, and in part by the Postgraduate Research and Practice Innovation Program of Jiangsu Province. *(Corresponding author: Ronger Lu.)*

Dongrui Di, Binglin Zhang, and Jiaying Wang are with the Department of Physics, Nanjing Tech University, Nanjing 211816, China (e-mail: 18890345219@163.com; 13994874479@163.com; wjy1195@163.com).

Ronger Lu is with the Department of Physics, Nanjing Tech University, Nanjing 211816, China, and also with the National Laboratory of Solid State Microstructures, Nanjing University, Nanjing 210093, China (e-mail: luronger@njtech.edu.cn).

Digital Object Identifier 10.1109/JPHOT.2023.3267237

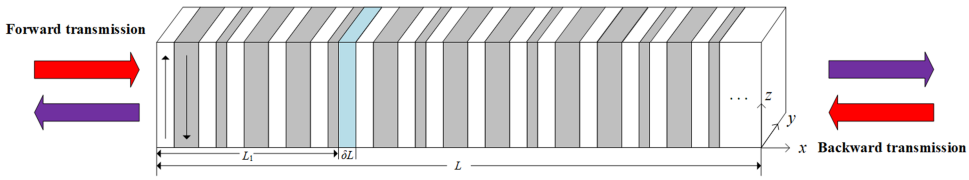

Fig. 1. A schematic of the forward and backward THG processes in the NPC with a defect embedded.

crystal, like LN, can be used as the material platform. The structure schematic is shown in Fig. 1, where the up and down arrows represent the domain poling directions, the white part represents the positive domain, the gray part represents the negative domain, and the blue part is the embedded defect. Supposing the whole length of the NPC is L, a defect with a width of δL is embedded at the position $x = L_1$.

The nonreciprocity of the THG process is slightly more complex than that of the single SHG process, because it simultaneously includes the SHG, the sum frequency generation (SFG), and the difference frequency generation (DFG) processes. In general, the coupled wave equations for the THG process in the NPC can be written as [24]:

$$\begin{cases} \frac{dA_1}{dx} = -iK_1A_2A_1^*f(x)\exp(-i\Delta k_1 x) \\ \qquad\quad - iK_2A_3A_2^*f(x)\exp(-i\Delta k_2 x) \\ \frac{dA_2}{dx} = -i\frac{1}{2}K_1A_1^2f(x)\exp(i\Delta k_1 x) \\ \qquad\quad - iK_2A_3A_1^*f(x)\exp(-i\Delta k_2 x) \\ \frac{dA_3}{dx} = -iK_2A_1A_2f(x)\exp(i\Delta k_2 x) \end{cases} \tag{1}$$

where A_1, A_2 ,A_3 refer to the field distributions of the fundamental wave (FW), the second harmonic wave (SHW), and third harmonic wave (THW), respectively. K_1 and K_2 are nonlinear coupling coefficients of SHG and SFG, respectively and $f(x)$ represents the structure function of the NPC. $\Delta k_1 = k_2 - 2k_1$ is the phase mismatching in the SHG process, where $k_1$and k_2 are correspondingly the wave vectors of FW and SHW. $\Delta k_2 = k_3 - k_2 - k_1$ is the phase mismatching in the SFG process, where k_3 is the wave vector of THW [25]. For THW, NPCs need to provide two reciprocal vectors G_1 and G_2, which are to compensate for phase mismatches in the SHG and SFG processes, where $G_1 = \Delta k_1$ and $G_2 = \Delta k_2$, respectively.

Due to the introduction of a defect, we can divide the crystal structure into three parts.

For the first section of the NPC ($0 \sim L_1$), in order to achieve quasi-phase matching (QPM)for both SHG and SFG processes, the NPC structure function satisfies

$$f(x) = \mathrm{sgn}(\cos G_1 x + \cos G_2 x) \tag{2}$$

The Fourier coefficients g_1, g_2 of SHG and SFG can be obtained by Fourier transform of NPC structure function:

$$\begin{cases} g_1 = \frac{1}{L}\int_0^L f(x)\exp(-iG_1 x)dx \\ g_2 = \frac{1}{L}\int_0^L f(x)\exp(-iG_2 x)dx \end{cases} \tag{3}$$

Under these circumstances, (1) can be further written in the following simplified form:

$$\begin{cases} \frac{dA_1}{dx} = -iK'^*_1A_2A_1^* - iK'^*_2A_3A_2^* \\ \frac{dA_2}{dx} = -\frac{1}{2}iK'_1A_1^2 - iK'^*_2A_3A_1^* \\ \frac{dA_3}{dx} = -iK'_2A_1A_2 \end{cases} \tag{4}$$

where

$$\begin{cases} K'_1 = K_1\,|g_1| \\ K'_2 = K_2\,|g_2| \end{cases} \tag{5}$$

For the second section ($L_1 \sim L_1 + \delta L$), the NPC structure function satisfies:

$$f(x) = \mathrm{sgn}(\cos G_1 L_1 + \cos G_2 L_1) \tag{6}$$

Phase shifts (denoted as $\Delta\varphi_1$and $\Delta\varphi_2$) are generated by the embedded defect for the SHG and SFG processes, which are given by the following equation:

$$\begin{cases} \Delta\varphi_1 = \delta L \cdot \Delta k_1 \\ \Delta\varphi_2 = \delta L \cdot \Delta k_2 \end{cases} \tag{7}$$

From (7), we can also obtain the relationship between phase shifts of SHG and SFG processes, namely $\Delta\varphi_2 = \Delta\varphi_1\frac{\Delta k_2}{\Delta k_1}$.

For the third section ($L_1 + \delta L \sim L$), the structure function satisfies

$$f(x) = \mathrm{sgn}\left[\cos G_1(x - \delta L) + \cos G_2(x - \delta L)\right] \tag{8}$$

The simplified coupled wave equations under the QPM conditions are similar with (4), which can be written as

$$\begin{cases} \frac{dA_1}{dx} = -iK''^*_1A_2A_1^* - iK''^*_2A_3A_2^* \\ \frac{dA_2}{dx} = -\frac{1}{2}iK''_1A_1^2 - iK''^*_2A_3A_2^* \\ \frac{dA_3}{dx} = -iK''_2A_1A_2 \end{cases} \tag{9}$$

With the influence of the structure of second section, K''_1, K''_2 here satisfy the following relations:

$$\begin{cases} K''_1 = K'_1\exp(-i\Delta\varphi_1) \\ K''_2 = K'_2\exp(-i\Delta\varphi_2) \end{cases} \tag{10}$$

It can be seen from the expressions that the magnitudes of K''_1 and K''_2 remain unchanged, but the arguments change with the width of the defect, as is shown in Fig. 2.

In order to illustrate the correctness of the simplified (4) and (9), the harmonic evolution diagrams are drawn according to the original (1) and the simplified (4) and (9), respectively. As shown in Fig. 3, in which $\Delta\varphi_1 = 0.8\pi$. The dotted line in the

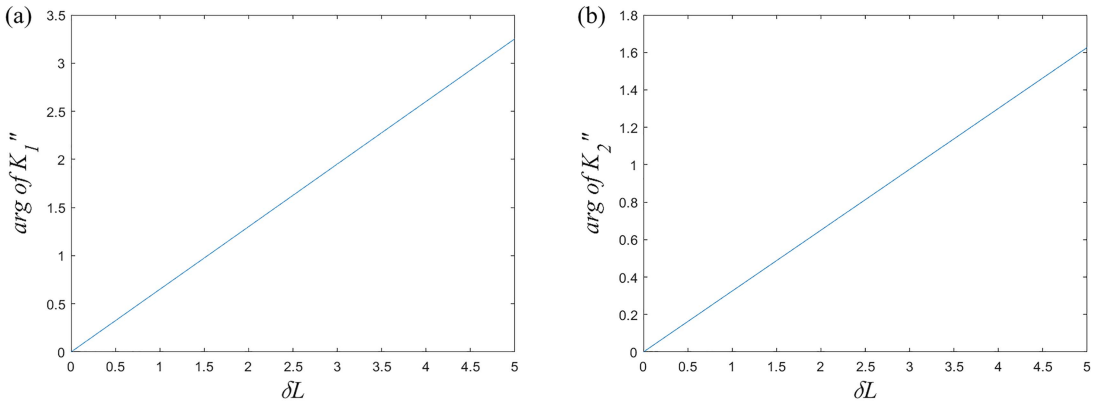

Fig. 2. Relationships between the arguments of the coupling coefficients and the width of the defect δL. (a) The argument of K_1'' , (b) the argument of K_2''.

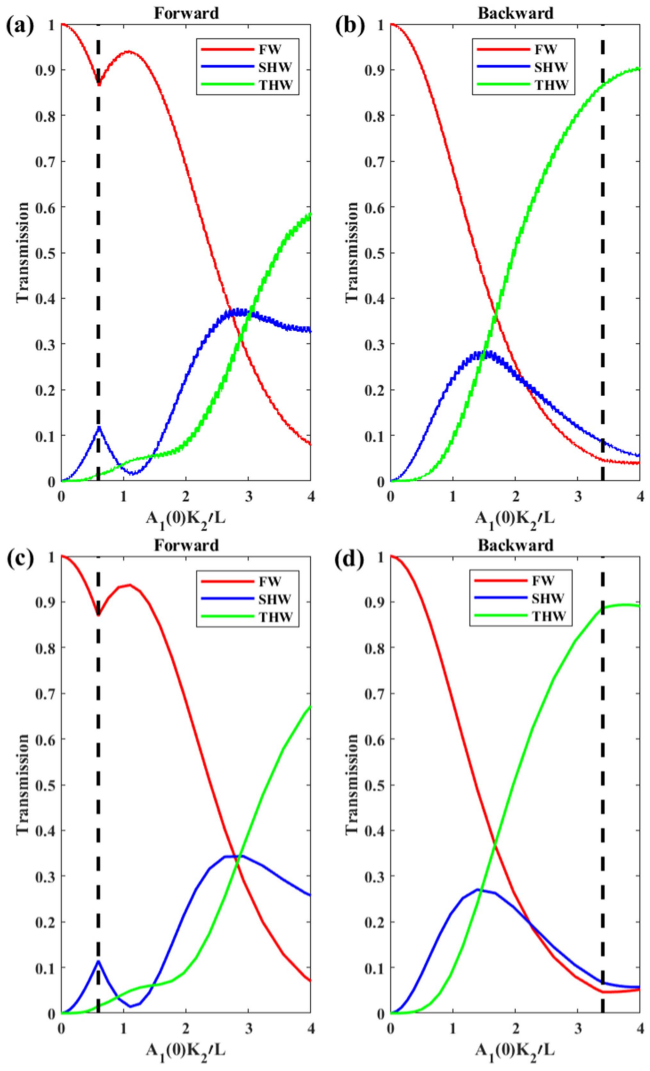

Fig. 3. The forward and backward evolution diagrams of the FW, SHW, THW in the NPC structure with a defect embedded. (a) And (b) are calculated from the original equation, (c) and (d) are calculated from the simplified equation. The dotted line in the figure refers to the position of the defect. In this calculation, $A_1(0)K_2'L_1 = 0.6$, $A_1(0)K_2'L = 4$, and the phase shift for SHG caused by the defect is 0.8π.

figure is the position where the defect is introduced. For the forward transmission process, the intensities of the FW, SHW, and THW at the position of $x = L$ are about 0.08, 0.33, and 0.58 calculated by the original equations [see Fig. 3(a)] while about 0.07, 0.26, and 0.67 calculated by the simplified equations [see Fig. 3(c)]. For the backward transmission process, the intensities of the FW, SHW, and THW at the position of $x = 0$ are about 0.04, 0.06, and 0.90 calculated by the original equations [see Fig. 3(b)] while about 0.05, 0.06, and 0.89 calculated by the simplified equations [see Fig. 3(d)]. The energy oscillation is a result of the competition between SHG, SFG and DFG. when the SHG process dominates, the SHW is stronger than the THW. Similarly, when the SFG process dominates, the THW is stronger than the SHW. When the DFG process dominates, it will result in a decrease of the THW and an increase of the FW and the SHW. The evolution trends calculated by the two coupled wave equations match well in both forward and backward transmission processes. This further proves that it is correct to simplify the original equations to (4) and (9), which is convenient for the follow-up discussions of nonreciprocity.

III. Discussions About the Nonreciprocal Response for THG

In general, the coupled wave equations for the THG process cannot be solved analytically in this NPC structure with a defect, and the small signal approximation is not applicable. Therefore, the nonreciprocity properties for the THW is usually solved by numerical methods. The nonreciprocity parameter can be defined as:

$$P = \frac{|I^+ - I^-|}{I^+ + I^-} \tag{11}$$

where I^+ and I^- represent the forward and backward output intensities of THW, respectively.

It is reported that the coupling coefficient ratio ($\tau = K_1/K_2$) greatly effects the maximum conversion efficiency of THW, and the optimal coupling coefficient ratio is about 0.8858 corresponding to the optimal matching condition [26]. The maximum THW conversion efficiency can be obtained when $\tau = 0.8858$,

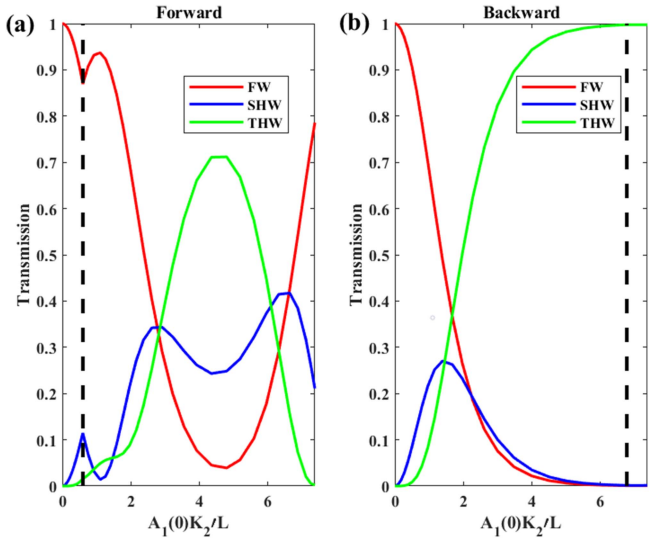

Fig. 4. In the NPC, the forward and backward wave evolution diagrams when $K_1/K_2 = 0.8858$. The dotted line in the figure refers to the position of the defect. The main calculation parameters are $\Delta\varphi_1 = 0.8\pi$, $A_1(0)K_2'L_1 = 0.6$, $A_1(0)K_2'L = 7.387$.

the energy can be transferred completely to the THW. Therefore, we adopt the condition $K_1/K_2 = 0.8858$ to design the NPC structure. Under this condition, the calculated intensities of the FW, SHW, and THW for the forward and backward transmission processes are shown in Fig. 4.

For the forward transmission process [see Fig. 4(a)], the FW, SHW, and THW show an oscillatory variation, which are strongly influenced by the defect as it is located close to the left ($A_1(0)K_2'L_1 < 6$). For the backward transmission process [see Fig. 4(b)], the intensity of the FW decreases monotonously and the intensity of the SHW begins to decrease when it reaches the maximum value. After propagating a certain distance ($A_1(0)K_2'(L - L_1) = 6$), the intensities of the FW and the SHW both tend to 0 and the system energy is all converted to the THW. Thereafter, the defect has almost no effect on the final output of the THW. If we order $\tau = 0.8858$ and $A_1(0)K_2'(L - L_1) > 6$, then (11) can be simplified to

$$P = \frac{1 - I^+}{1 + I^+} \tag{12}$$

That is, if we want to achieve 100% nonreciprocal response, we need to make the forward THW output $I^+ = 0$. Obviously, the forward THW output is related to the normalized defect location $A_1(0)K_2'L_1$, the normalized total length of the NPC $A_1(0)K_2'L$, and the phase shift $\Delta\varphi_1$ introduced by the defect. Under some specific structure parameters shown in Fig. 4, this ideal complete nonreciprocity can be realized.

Fig. 5 shows the contour map of the nonreciprocity parameter P with the total NPC length $A_1(0)K_2'L$ and the defect $\Delta\varphi_1$, where $A_1(0)K_2'L_1 = 0.3\pi$ is a constant. Fig. 5(b) is a partly enlarged graph of Fig. 5(a). It can be seen from Fig. 5(b) that the nonreciprocity parameter P is approximately periodically distributed when $\Delta\varphi_1$ takes a constant value. The closer to red in the figure, the value of P is closer to 1. It is meaningful in Fig. 5(b)

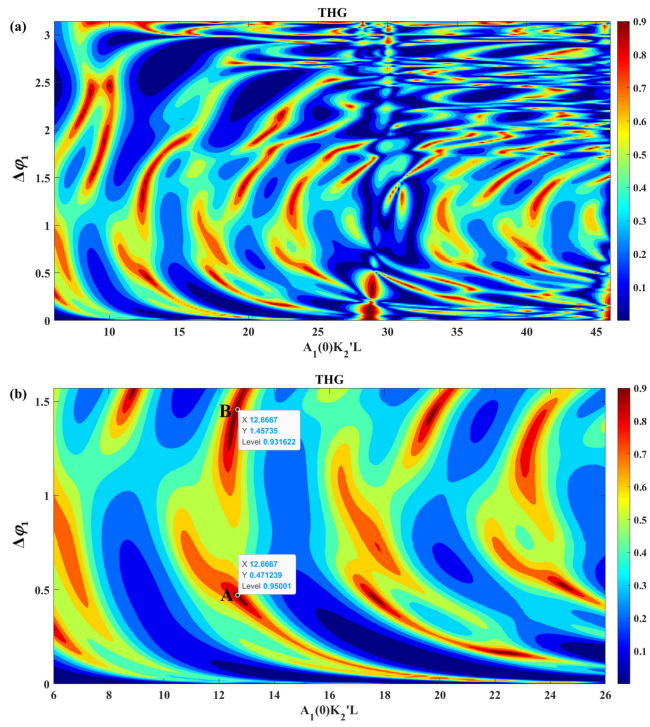

Fig. 5. The contour color map of THG nonreciprocity parameter *P*.

that the value of P at points A (12.67,0.47) and B (12.67,1.46) are greater than 0.9. This means that in practical applications, we do not need too long NPC structures, only $A_1(0)K_2'L = 12.6$, and a large value of P can be obtained by properly adjusting the phase shift.

For practical applications in a defective NPC structured on the LN, the nonlinear coefficient $d_{33} = 27pm/V$. If a 95% nonreciprocal contrast is required, that is $P = 0.95$, $A_1(0)K_2'L \approx 12.6667$ and $\Delta\varphi_1 \approx 0.47$ can be sketched by point 'A' in Fig. 5(b). The data show that if we set the FW (1560 nm) intensity to be 60 MW/cm^2, the needed total length is $L = 1.69$ cm, the required defect width is $\delta L = 0.72$ μm, and the defect position is $L_1 = 0.126$ cm. Similarly, if an 93% nonreciprocal contrast is required, the corresponding parameters can be obtained by the same method, shown by point 'B' in the figure. Discussions above have explained a universal design for nonreciprocal responses of THG in the defective NPCs. The maximum conversion efficiency required for this process is about 27%, which is comparable to values obtained in experiments in references [27], [28]. Thus, we believe it will be a more flexible and easier method to control the design of diodes.

IV. Conclusion

In conclusion, we have theoretically studied the nonreciprocity of THG process in NPCs with defects. We have calculated the forward and backward harmonic propagating processes from the original and the simplified coupled wave functions and they match well with each other. From the numerical results, an interesting circumstance that the forward THW output is 0, and the backward THW output is 1 can be achieved when specific

structure conditions are taken, thus we call it the complete nonreciprocity for THG. It can be found that nonreciprocity parameter of THG also has a periodicity to a certain extent, any target nonreciprocity can be obtained by adjusting the NPC length, the defect width and the defect position. These results may have potential applications in all-optical diodes, optical isolators, amplifiers, circulators and so on.

REFERENCES

[1] W. Jeon, O. Salicio, A. Chaker, P. Gonon, and C. Vallee, "Controlling the current conduction asymmetry of HfO_2 metal-insulator-metal diodes by interposing Al_2O_3 layer," *IEEE Trans. Electron. Devices*, vol. 66, no. 1, pp. 402–406, Jan. 2019.

[2] D. Matsuura, M. Shimizu, and H. Yugami, "High-current density and high-asymmetry MIIM diode based on oxygen-non-stoichiometry controlled homointerface structure for optical rectenna," *Sci. Rep.*, vol. 9, pp. 1–7, Dec. 2019.

[3] K. Shiga et al., "Electrical transport properties of gate tunable graphene lateral tunnel diodes," *Japanese J. Appl. Phys.*, vol. 59, Jun. 2020, Art. no. SIID03.

[4] S. Liu, R. Shao, S. Ma, L. Zhang, and S. Zhang, "Non-Hermitian skin effect in a non-Hermitian electrical circuit," *Research*, vol. 2021, pp. 1–9, 2021.

[5] Z. Chen et al., "Efficient nonreciprocal mode transitions in spatiotemporally modulated acoustic metamaterials," *Sci. Adv.*, vol. 7, no. 45, 2021, Art. no. eabj1198.

[6] M. Kulishov, J. M. Laniel, N. Bélanger, J. Azaña, and D. V. Plant, "Nonreciprocal waveguide Bragg gratings," *Opt. Exp.*, vol. 13, no. 8, pp. 3068–3078, 2005.

[7] L. Feng et al., "Nonreciprocal light propagation in a silicon photonic circuit," *Science*, vol. 333, no. 6043, pp. 729–733, 2011.

[8] X.-X. Hu et al., "Noiseless photonic non-reciprocity via optically-induced magnetization," *Nature Commun.*, vol. 12, no. 1, 2021, Art. no. 2389.

[9] M. Krause, H. Renner, and E. Brinkmeyer, "Optical isolation in silicon waveguides based on nonreciprocal Raman amplification," *Electron. Lett.*, vol. 44, no. 11, p. 1, May 2008.

[10] M. Lawrence and J. A. Dionne, "Nanoscale nonreciprocity via photon-spin-polarized stimulated Raman scattering," *Nature Commun.*, vol. 10, Jul. 2019, Art. no. 2397.

[11] E. A. Kittlaus, N. T. Otterstrom, P. Kharel, S. Gertler, and P. T. Rakich, "Non-reciprocal interband Brillouin modulation," *Nature Photon.*, vol. 12, no. 10, pp. 613–619, Oct. 2018.

[12] X. Zeng et al., "Nonreciprocal vortex isolator via topology-selective stimulated Brillouin scattering," *Sci. Adv.*, vol. 8, no. 42, Oct. 2022, Art. no. eabq6064.

[13] A. Lopez-Gil, X. Angulo-Vinuesa, A. Dominguez-Lopez, S. Martin-Lopez, and M. Gonzalez-Herraez, "Exploiting nonreciprocity in BOTDA systems," *Opt. Lett.*, vol. 40, no. 10, pp. 2193–2196, May 2015.

[14] N. T. Otterstrom et al., "Resonantly enhanced nonreciprocal silicon Brillouin amplifier," *Optica*, vol. 6, no. 9, pp. 1117–1123, Sep. 2019.

[15] T. Shui, W. X. Yang, M. T. Cheng, and R. K. Lee, "Optical nonreciprocity and nonreciprocal photonic devices with directional four-wave mixing effect," *Opt. Exp.*, vol. 30, no. 4, pp. 6284–6299, Feb. 2022.

[16] Y. Z. Zhang et al., "Phase control of optical nonreciprocity in photonic bandgap four-wave mixing," *IEEE Photon. J.*, vol. 8, no. 3, Jun. 2016, Art. no. 4501311.

[17] H. Wang et al., "Scanning nonreciprocity spatial four-wave mixing process in moving photonic band gap," *Laser Phys.*, vol. 27, no. 3, Mar. 2017, Art. no. 035402.

[18] K. Wang et al., "Four-wave-mixing-based silicon integrated optical isolator with dynamic non-reciprocity," *IEEE Photon. Technol. Lett.*, vol. 28, no. 16, pp. 1739–1742, Aug. 2016.

[19] H. Kurt, D. Yilmaz, A. E. Akosman, and E. Ozbay, "Asymmetric light propagation in chirped photonic crystal waveguides," *Opt. Exp.*, vol. 20, no. 18, pp. 20635–20646, Aug. 2012.

[20] X. S. Qian et al., "Electro-optic tunable optical isolator in periodically poled $LiNbO_3$," *J. Appl. Phys.*, vol. 109, no. 5, Mar. 2011, Art. no. 053111.

[21] R. Lu et al., "Analytical investigation of nonreciprocal response in 1D nonlinear photonic crystals," *Sci. Rep.*, vol. 7, Jul. 2017, Art. no. 6579.

[22] K. Gallo and G. Assanto, "All-optical diode based on second-harmonic generation in an asymmetric waveguide," *J. Opt. Soc. Amer. B*, vol. 16, no. 2, pp. 267–269, Feb. 1999.

[23] K. Gallo, G. Assanto, K. R. Parameswaran, and M. M. Fejer, "All-optical diode in a periodically poled lithium niobate waveguide," *Appl. Phys. Lett.*, vol. 79, no. 3, pp. 314–316, Jul. 2001.

[24] C. Zhang, Y. Y. Zhu, S. N. Zhu, and N. B. Ming, "Coupled quasi-phase-matched high-order harmonic generation," *J. Opt. A: Pure Appl. Opt.*, vol. 3, no. 5, pp. 317–320, Sep. 2001.

[25] S. Zhu, Y. Y. Zhu, and N. B. Ming, "Quasi-phase-matched third-harmonic generation in a quasi-periodic optical superlattice," *Science*, vol. 278, no. 5339, pp. 843–846, Oct. 1997.

[26] C. Zhang et al., "Crucial effects of coupling coefficients on quasi-phase-matched harmonic generation in an optical superlattice," *Opt. Lett.*, vol. 25, no. 7, pp. 436–438, Apr. 2000.

[27] C.-W. Hsu, J.-Y. Lai, and S.-D. Yang, "Quasi-phase-matching efficiency optimization for coupled second-order nonlinear processes," *IEEE Photon. Technol. Lett.*, vol. 31, no. 21, pp. 1721–1724, Nov. 2019.

[28] K. Zhang and J. M. Wang, "Efficient single-pass third-harmonic generation from 1560 nm to 520 nm for pumping doubly-resonant OPO," *J. Modern Opt.*, vol. 64, no. 15, pp. 1510–1518, 2017.